2014 Madrid Conference on Applied Mathematics in honor of Alfonso Casal,
Electronic Journal of Differential Equations, Conference 22 (2015), pp. 99–109.
ISSN: 1072-6691. URL: http://ejde.math.txstate.edu or http://ejde.math.unt.edu
ftp ejde.math.txstate.edu

COMMENTS ON MULTIPLE OSCILLATORY SOLUTIONS IN SYSTEMS WITH TIME-DELAY FEEDBACK

MICHAEL STICH

Dedicated Alfonso Casal on his 70th birthday

Abstract. A complex Ginzburg-Landau equation subjected to local and global time-delay feedback terms is considered. In particular, multiple oscillatory solutions and their properties are studied. We present novel results regarding the disappearance of limit cycle solutions, derive analytical criteria for frequency degeneration, amplitude degeneration, and frequency extrema. Furthermore, we discuss the influence of the phase shift parameter and show analytically that the stabilization of the steady state and the decay of all oscillations (amplitude death) cannot happen for global feedback only. Finally, we explain the onset of traveling wave patterns close to the regime of amplitude death.

1. Introduction

It is well-known that the spatiotemporal dynamics of reaction-diffusion systems in the vicinity of a Hopf bifurcation are described by the complex Ginzburg-Landau equation [5, 7]. In the relevant case of a supercritical Hopf bifurcation, the primary solution of this system is a stable limit cycle appearing at the Hopf bifurcation. However, in some parameter range (if the Benjamin-Feir-Newell criterion $1+\alpha\beta < 0$ is fulfilled), the oscillations in the spatially-extended system may be unstable, a phenomenon that is induced by the diffusive coupling and that is therefore genuine to a system with spatial degrees of freedom.

During many years, considerable efforts have been made to understand this type of chaotic behavior and to apply methods to suppress this kind of turbulence and replace it by simpler, more regular dynamics. Consequently, control of chaotic states in nonlinear systems is a wide field of research that we cannot review here [9]. In the context of the reaction-diffusion systems, the introduction of forcing terms or global feedback terms have been shown to be efficient ways to control turbulence [8].

Global feedback methods, where a spatially independent quantity (in many cases a spatial average of a space-dependent quantity) is coupled back to the system dynamics, have attracted much attention since in many cases the equations are easier

2010 *Mathematics Subject Classification.* 35K57, 35B10, 35Q92.
Key words and phrases. Pattern formation; reaction-diffusion system; control.

Published November 20, 2015.

to analyse and to be implemented experimentally [9]. Nevertheless, local methods have gained interest in recent years since they allow to access other solutions of the systems and may also be implemented, such as in the light-sensitive BZ reaction or in neurophysiological experiments with spatial arrays of electrodes.

Feedback methods with an explicit time delay widen the range of possibilities of control that can be applied to the system and provide the researcher with an additional adjustable parameter. On the level of the mathematical description, the model equations become delay differential equations.

Motivated by previous works [2, 3, 4, 10, 11, 12], the complex Ginzburg-Landau equation subjected to a time-delay feedback with local and global terms is studied here. Extensive simulations showed the range of patterns that can be stabilized as function of the local and global feedback terms [12]. If the feedback is global, local, or a combination of both, uniform oscillations, the basic temporally-periodic solution of a system close to a Hopf bifurcation, can be stabilized. In [10], we studied the homogeneous periodic and the homogeneous stationary (amplitude death) solutions from an analytical point of view, performed linear stability analysis and derived the limiting curves of the stability regions. In this contribution, we dwell into previously overlooked features of this model, that however have interesting and important consequences for future applications.

2. The model system

Reaction-diffusion systems can display various types of oscillatory dynamics. However, close to a supercritical Hopf bifurcation, all such systems are described by the complex Ginzburg-Landau equation (CGLE) [1],

$$\frac{\partial A}{\partial t} = (1 - \mathrm{i}\omega)A - (1 + \mathrm{i}\alpha)|A|^2 A + (1 + \mathrm{i}\beta)\Delta A, \tag{2.1}$$

where A is the complex oscillation amplitude, ω the linear frequency parameter, α the nonlinear frequency parameter, β the linear dispersion coefficient, and Δ the Laplacian operator. For $1 + \alpha\beta < 0$ (the Benjamin-Feir-Newell criterion), the homogeneous periodic solution $A_u = \mathrm{e}^{-\mathrm{i}(\omega+\alpha)t}$ is unstable and a regime of spatiotemporal chaos is observed.

The CGLE for a one-dimensional medium with a combination of local and global time-delayed feedback has been introduced in [12] and reads

$$\begin{aligned} \frac{\partial A}{\partial t} &= (1 - \mathrm{i}\omega)A - (1 + \mathrm{i}\alpha)|A|^2 A + (1 + \mathrm{i}\beta)\frac{\partial^2 A}{\partial x^2} + F, \\ F &= \mu \mathrm{e}^{\mathrm{i}\xi}\left[m_l(A(x, t-\tau) - A(x,t)) + m_g(\bar{A}(t-\tau) - \bar{A}(t))\right], \end{aligned} \tag{2.2}$$

where

$$\bar{A}(t) = \frac{1}{L}\int_0^L A(x,t)\,\mathrm{d}x \tag{2.3}$$

denotes the spatial average of A over a one-dimensional medium of length L. We assume Neumann boundary conditions

$$\frac{\partial A}{\partial x}\Big|_{0,L} = 0, \tag{2.4}$$

which is a reasonable choice for reaction-diffusion systems. The parameter μ describes the feedback strength and ξ characterizes a phase shift between the feedback and the current dynamics of the system. The parameters m_g and m_l denote the

global and local contributions to the feedback, respectively. If $m_l = 0$, the case of global time-delay feedback is retrieved [2].

As result of extensive simulations, many different spatiotemporal patterns occurring in this system have been identified [12]. Besides the basic, homogeneous periodic solution, we mention standing waves, traveling waves, amplitude death, complex localized patterns, and spatiotemporal chaos. The stabilization of an homogeneous periodic solution and amplitude death have been considered in [10]. First, we introduce the homogeneous periodic solution.

3. Homogeneous periodic solution

The feedback-induced, homogeneous periodic solution is given by

$$A_0(t) = \rho \mathrm{e}^{-\mathrm{i}\Omega t}. \tag{3.1}$$

It is a solution of (2.2) with the amplitude and frequency given by

$$\rho = \sqrt{1 + \mu(m_g + m_l)\chi_1}, \tag{3.2a}$$

$$\Omega = \omega + \alpha + \mu(m_g + m_l)(\alpha\chi_1 - \chi_2)\,. \tag{3.2b}$$

Here, $\chi_{1,2}$ denote effective modulation terms that can be positive or negative. They arise from the feedback and hence depend on ξ and τ,

$$\chi_1 = \cos(\xi + \Omega\tau) - \cos\xi, \tag{3.3a}$$

$$\chi_2 = \sin(\xi + \Omega\tau) - \sin\xi. \tag{3.3b}$$

Equations (3.2a),3.2b do not explicitly depend on ρ, only on Ω. However, no explicit analytic solution for (3.2b) can be given because $\chi_{1,2}$ also depend on Ω. Nevertheless, the solution can be computed using root-finding algorithms, as done in [10].

In the absence of feedback ($\mu = 0$), the standard solution for the CGLE is recovered: $\rho_0 = 1$, $\Omega_0 = \omega + \alpha$. Applying the parameters used in [12], and in particular $\omega = 2\pi - \alpha$, the period of the oscillations is chosen to be $T_0 = 2\pi/\Omega_0 = 1$. As already mentioned, this solution is unstable for $1 + \alpha\beta < 0$, also assumed here. We assume $m_l + m_g = 1$, but a generalization to other combinations of m_l and m_g is straightforward [4].

4. Existence of multiple oscillatory solutions

The multiplicity of uniform oscillatory solutions is a direct consequence of the above-mentioned Equation (3.2b) and which is an established fact for various versions of the CGLE at least since [2]. Surprisingly, the shape of the curves that describe these equations has not been studied in more detail, which will be done here.

Following [10], we show how multiplicity of solutions is introduced as we vary τ and μ as control parameter. If the feedback strength is small and we vary τ, the oscillation frequency is not constant, but remains relatively close to the value of the frequency of oscillations for $\mu = 0$. However, if the value of μ is larger than a critical threshold, there is an interval of τ for which the (3.2b) has three solutions, the center one being unstable always. This is shown in Figure 1(a). If an even larger value of μ is chosen, the interval of τ in which multiplicity of solutions occurs becomes larger.

It is important to note that we consider small to medium values of μ, up to $\mu \approx 2$ (as in [10]). The rationale behind this is that we are interested in the constructive interplay between the terms on the right-hand side of (2.2), not in the case where the feedback terms will strongly dominate the native dynamics.

The multiplicity of solutions is a direct consequence of the equation for the frequency, (3.2b). However, the equation for the amplitude, (3.2a), has also to be taken into account. In particular, the value of the amplitude has to take a positive value if it should correspond to an actual oscillation. In Figure 1(b), we show the amplitudes and periods of the solutions for a fixed μ. The solid curves represent the periods, and the dashed curves the amplitudes. Color codes for corresponding parts of the solution. Let us consider first large values of τ. The blue (thick) curve represents the oscillation with a relatively high frequency and large amplitude. Around $\tau \approx 1.06$, we enter the regime of birhythmicity, as also red (upper) and green (middle) branches appear, green (red) referring to the unstable (stable) branch. Our focus here is on the amplitude and we see that the limit cycle corresponding to the unstable oscillations disappears close to $\tau \approx 0.87$. Furthermore, around $\tau \approx 0.84$, the stable high-frequency solution disappears as well. This means that although we are in an apparent regime of birhythmicity due to the multiplicity of frequency solution, actually below $\tau \approx 0.84$ only the low-frequency solution is left as unique solution. The parts of the frequency curves that actually do not correspond to any existing limit cycle solution are marked as black.

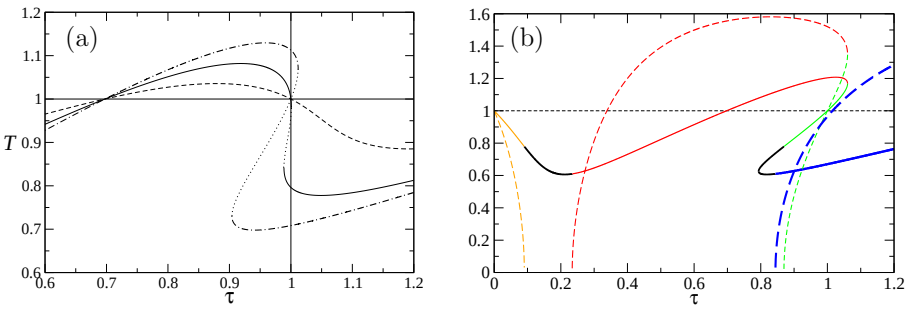

FIGURE 1. (a) The period of oscillations as determined by (3.2b) as a function of τ for $\mu = 0.3$ (dashed), $\mu = 0.66$ (solid), $\mu = 1.0$ (dotted-dashed). (b) Periods (solid) and amplitudes (dashed) as a function of τ are shown for $\mu = 1.5$. For more information see text. The other parameters are $\alpha = -1.4$, $\omega = 2\pi - \alpha$, $\xi = \pi/2$.

Below $\tau \approx 0.79$, the frequency solution is again single-valued until around $\tau \approx 0.23$ even that solution disappears as the amplitude of the oscillations approaches zero. Only for τ below 0.09, we observe again a limit cycle. The finite interval of τ for which no limit cycle is found and the stationary state is stabilized is called amplitude death. For this model, it has been studied in [10] and we show some novel results below.

Let us now consider again the frequency equation for a larger range of τ. In Figure 2(a) we show the results for three values of μ: While for the smallest feedback strength there is no multiplicity around $\tau \approx 1$, there is actually a range around $\tau \approx 2$ where this is found. The central observation here is that the interval sizes

where multiplicity is found become larger as τ increases and that these intervals are located around $\tau \approx nT_0$. As we go to larger τ, the branches become more and more inclined such that also for a fixed τ, multiplicity of more than 3 solutions is possible. For example, for $\mu = 1.5$ and $\tau = 3.0$ there are 5 frequency solutions (whether all of them correspond to valid limit cycle solutions has not been checked here). Therefore, both, increasing τ or μ leads to an increase of the number of frequency solutions.

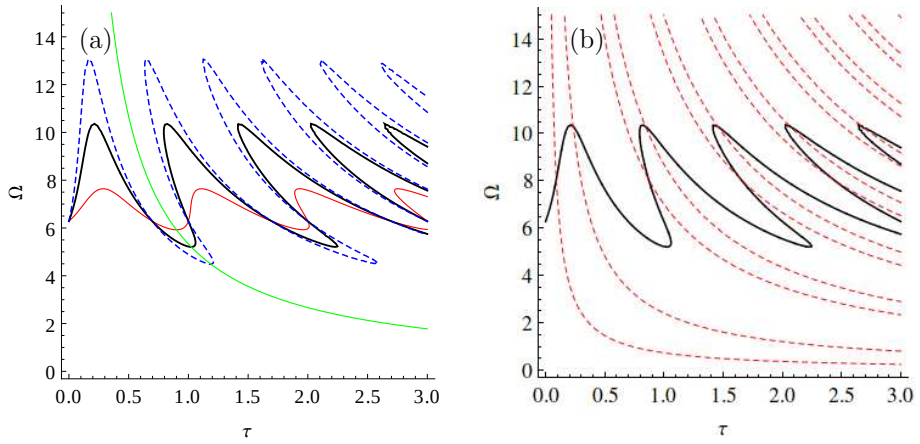

FIGURE 2. (a) Frequency as a function of τ for $\mu = 0.5$ (red thin curve), $\mu = 1.5$ (black solid curve), $\mu = 2.5$ (blue dashed curve). (b) Frequency as a function of τ for $\mu = 1.5$ (black solid curve) and the curves for which $\rho = 0$ (red dashed). The black curve enclosed by the first and second red curves (from left) denotes the first area where no oscillation is possible. The next area is defined by where the black curve is enclosed by the third and fourth red curves, etc. The other parameters are as in Figure 1.

Frequency degeneration. Another observation to make in this figure is that the curves for different μ intersect in the same points. Let us calculate their values through analysis of (3.2b). First, we clarify for which τ the period of the oscillations coincides with the one of uniform oscillations in the absence of feedback.

Case 1: $\tau = 0$. Then

$$\Omega(\tau = 0) = \omega + \alpha = \Omega_0. \tag{4.1}$$

Case 2: $\tau = n \cdot 2\pi/\Omega$ with $n = 1, 2, \ldots$. Then

$$\chi_1 = \cos\left(\xi + \Omega\frac{2\pi n}{\Omega}\right) - \cos\xi = \cos(\xi + 2\pi n) - \cos\xi = 0, \tag{4.2a}$$

$$\chi_2 = \sin\left(\xi + \Omega\frac{2\pi n}{\Omega}\right) - \sin\xi = \sin(\xi + 2\pi n) - \sin\xi = 0, \tag{4.2b}$$

and therefore

$$\Omega = \omega + \alpha + \mu(m_l + m_g)(\alpha\chi_1 - \chi_2) = \omega + \alpha = \Omega_0. \tag{4.3}$$

Therefore, the value of τ is actually:

$$\tau = \frac{2\pi n}{\Omega_0} = \frac{2\pi n}{\omega + \alpha}. \tag{4.4}$$

Case 2 includes Case 1 if we allow for $n = 0$. We call this value of τ:

$$\tau_0^* = nT_0, \tag{4.5}$$

for $n = 0, 1, 2, \ldots$.

Case 3: Another – and more interesting – possibility to obtain $\Omega \neq \Omega(\mu)$ (and therefore $\Omega = \Omega_0$) is to ask for

$$\alpha\chi_1 - \chi_2 = 0, \tag{4.6}$$

where we require $\alpha \neq 0$. First we write

$$\chi_1 = \cos(\xi + \Omega\tau) - \cos\xi = -2\sin\Big(\frac{2\xi + \Omega\tau}{2}\Big)\sin\Big(\frac{\Omega\tau}{2}\Big), \tag{4.7a}$$

$$\chi_2 = \sin(\xi + \Omega\tau) - \sin\xi = 2\sin\Big(\frac{\Omega\tau}{2}\Big)\cos\Big(\frac{2\xi + \Omega\tau}{2}\Big), \tag{4.7b}$$

and therefore

$$\tan\Big(\xi + \frac{\Omega\tau}{2}\Big) = -\frac{1}{\alpha}. \tag{4.8}$$

The cases where this reduction cannot be made correspond to the cases discussed above. Since we also know that $\Omega = \Omega_0$, we can reformulate and give an explicit expression for τ, denoted as:

$$\tau_1^* = \frac{1}{\omega + \alpha}\Big(2\arctan\big(-\frac{1}{\alpha}\big) - 2\xi + 2\pi n\Big), \tag{4.9}$$

with $n = 0, \pm 1, \pm 2, \ldots$ (but restricted to results with $\tau_1^* > 0$). For the parameters used in Figure 1, the first intersection point lies at $\tau \approx 0.69$ and corresponds to the solution with $n = 1$.

At this point we can search more generally for those values of $\tau_1 \neq \tau_2$, for which $\Omega_1 = \Omega_2 = \Omega$. A calculation analogous to the one above yields

$$\tan\Big(\xi + \frac{\Omega(\tau_1 + \tau_2)}{2}\Big) = -\frac{1}{\alpha}. \tag{4.10}$$

We leave the result in this form since in the general case we do not have an analytical expression for Ω. But for $\tau_2 = 0$ (and therefore $\Omega = \Omega_0$) we recover Case 3.

Extrema of the frequency curve. We can obtain the extrema of the frequency curve $\Omega(\tau)$ through implicit differentiation. After some transformations, the condition $d\Omega/d\tau = 0$ yields for non-zero α and non-zero μ the expression

$$\Omega\tau = \arctan\big(-\frac{1}{\alpha}\big) - \xi \pm n\pi, \tag{4.11}$$

where for our set of parameters ($\xi = \pi/2$, $\alpha = -1.4$) the first maximum corresponds to $n = 1$ and the first minimum to $n = 2$. Maxima and minima are obtained by (4.11) alternatingly. As example, in Figure 2(a) we show the hyperbola for the first minimum. Note that again this curve does not depend on μ.

Condition for vanishing amplitude. As we have already seen in Figure 1(b) that the amplitude of the oscillations can vanish, we evaluate (3.2a) in order to find an analytic criterion. The condition $\rho = 0$ yields two expressions:

$$\Omega\tau = \arccos\Big(\cos\xi - \frac{1}{\mu(m_l + m_g)}\Big) - \xi \pm 2\pi n, \tag{4.12a}$$

$$\Omega\tau = -\arccos\Big(\cos\xi - \frac{1}{\mu(m_l + m_g)}\Big) + \xi \pm 2\pi n, \tag{4.12b}$$

with $n = 0, 1, 2, \dots$ and restricted to $\tau > 0$ and $\Omega \neq 0$. These functions are shown in Figure 2(b) as dashed curves. Where these curves intersect with the curve for the period (solid curve), we find the limits where $\rho = 0$. For example, the interval where amplitude death is observed is found in between the first and second dashed curve (counted from left). For this interval, the lower bound is given by the first expression for $n = 0$, and the upper bound by the second expression for $n = 1$. The second interval (lying in the birhythmicity area) is limited by the curves given for $n = 2$ and $n = 3$, etc..

Amplitude degeneration. Above we have seen that besides $\tau_0^* = nT_0$ there is a τ_1^* where the oscillation frequency is independent of μ and identical to $2\pi/T_0$. We can check whether there is also a τ for which the amplitude is independent of μ and identical to $\rho_0 = 1$. A short inspection of Eq. (3.2a) shows that this is only the case for $\tau = \tau_0^*$, not for $\tau = \tau_1^*$. This means that although we can create different feedback-induced limit cycles with same frequency, we cannot create feedback-induced limit cycles with identical amplitudes.

Birhythmicity area revisited. With the obtained knowledge about the disappearance of limit cycle solutions within the apparent birhythmicity region, e.g., as shown in [10], we may have to correct the area where two stable limit cycles are found. This is shown in Figure 3(a). The thin black curves limits the area – on basis of the frequency equation (3.2b) – where three limit cycle solutions were believed to exist, two of them stable. The two new curves were derived from (4.12) and show the locus of $\rho = 0$ on the center branch (blue curve with circles) and on the high-frequency branch (red curve with squares). Since the center branch is unstable always, only to the left of the red branch the stability scenario can be modified effectively. Note that both curves end at $\mu = 1$ since $\xi = \pi/2$ and $m_l + m_g = 1$. Since the solution of uniform oscillation depends on the sum $m_l + m_g$, the shown curves do not depend on the specific choice of m_l. However, this changes once we consider *stability* of uniform oscillations. The stability curves depend on m_l and in Figure 3(a) we show as green dashed curves the stability limits (as derived in [10]) of the high-frequency solution for $m_l = 0.6$ (hence $m_g = 0.4$). The high-frequency solution becomes actually unstable *before* crossing the red curve, so that the stability scenario is effectively unchanged in this case. However, no extensive analysis is performed here, so we cannot exclude parameter values where a stable limit cycle disappears.

Influence of ξ. In previous work on that model [12, 10, 11], the parameter controlling the shift between the system dynamics and the feedback ξ has been taken the value $\pi/2$. Here, we want to study the influence it has on the shape of the frequency curve. This is displayed in Figure 3(b) for a fixed $\mu = 1$ for 8 values of ξ from 0 to $7\pi/4$. The first observation is that the oscillation frequency can

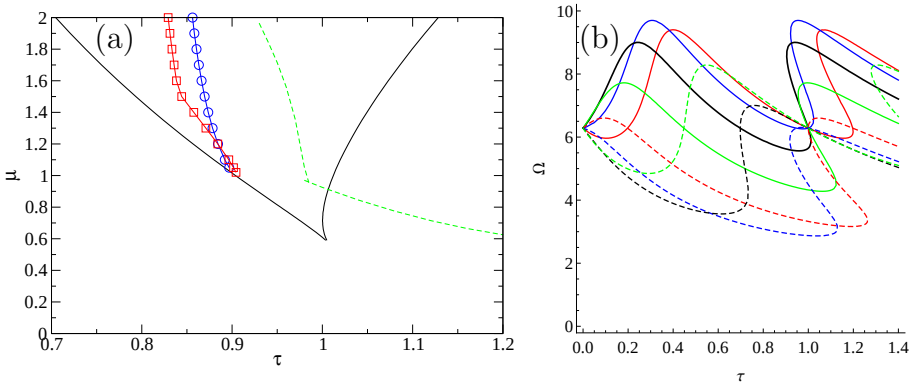

FIGURE 3. (a) Birhythmicity area for $\alpha = -1.4$, $\omega = 2\pi - \alpha$, $\xi = \pi/2$ and $m_l + m_g = 1$. The thin black curves that denote the limits of the multiplicity area for the frequency equation (3.2b), as shown in [10]. To the left of the blue curve (with circles), the center solution (always unstable) is absent, to the left of the red curve (with squares), the high-frequency solution. The green dashed curves show where the high-frequency solution becomes unstable (stable in the upper right area). (b) The frequency equation (3.2b) for $\mu = 1$ and for $\xi = 0$ to $\xi = 7\pi/4$ in steps of $\pi/4$ in order red, blue, black, green, then dashed red, dashed blue, dashed black, dashed green.

be tuned to be much larger than the native frequency Ω_0 over almost the whole range of τ, as for example for $\xi = \pi/4$ (blue curve). Inspection of (3.2b) shows that this also depends strongly on α. The second observation is that for a given ξ the curves $\Omega(\xi)$ and $\Omega(\xi + \pi)$ intersect where $\Omega = \Omega_0$. This reflects the fact that τ_1^* is invariant to a shift of $\xi \to \xi + n\pi$ (cf. (4.9)). This also implies that for a fixed τ a shift $\xi \to \xi + n\pi$ represents a switch from a low-frequency solution to a high-frequency solution (or vice versa). This is a slight over-simplification since the areas of existence of solutions do not match in general under such as shift (not to mention stability).

5. Amplitude death

Amplitude death represents a collective breakdown of oscillations and the simultaneous stabilization of a stationary state. Therefore, it can be studied by checking for the stability of the fixed point solution $\rho = 0$. Let us recall some results from [10]. By using a mode separation ansatz

$$A(x,t) = H(t) + A_+(t)e^{\mathrm{i}\kappa x} + A_-(t)e^{-\mathrm{i}\kappa x} \tag{5.1}$$

we obtain to lowest order in H and $A_\pm$

$$\dot{H} = (1 - \mathrm{i}\omega)H + \mu(m_l + m_g)e^{\mathrm{i}\xi}(H(t-\tau) - H(t)), \tag{5.2a}$$

$$\dot{A}_+ = (1 - \mathrm{i}\omega)A_+ - (1 + \mathrm{i}\beta)\kappa^2 A_+ + \mu m_l e^{\mathrm{i}\xi}(A_+(t-\tau) - A_+), \tag{5.2b}$$

$$\dot{A}_-^* = (1 + \mathrm{i}\omega)A_-^* - (1 - \mathrm{i}\beta)\kappa^2 A_-^* + \mu m_l e^{-\mathrm{i}\xi}(A_-^*(t-\tau) - A_-^*). \tag{5.2c}$$

These three equations are decoupled and can be studied independently. In order to investigate the linear stability of the state $H = 0$ with respect to uniform perturbations, we set

$$H = H_0 \exp(\lambda t), \tag{5.3}$$

with H_0 an initial amplitude and λ a complex eigenvalue. Inserting (5.3) into (5.2a), yields the following characteristic equation

$$\lambda = 1 - \mathrm{i}\omega + \mu(m_l + m_g)\mathrm{e}^{\mathrm{i}\xi}(\mathrm{e}^{-\lambda\tau} - 1). \tag{5.4}$$

This equation is equivalent to the amplitude death condition for a single Hopf oscillator and can be solved with the Lambert W function or numerically. Note that the homogeneous mode behaves the same for all relative weights between local and global feedback as long as the sum $m_l + m_g$ is constant (as assumed here).

We now turn to the inhomogeneous modes with wavenumber κ. Since (5.2b) and (5.2c) are decoupled and identical, it is sufficient to consider only one of them. Substituting the ansatz

$$A_+ = A_+^0 \exp(\lambda t) \tag{5.5}$$

into (5.2b), we obtain

$$\lambda = 1 - \mathrm{i}\omega - \kappa^2 - \mathrm{i}\beta\kappa^2 + \mu m_l \mathrm{e}^{\mathrm{i}\xi}(\mathrm{e}^{-\lambda\tau} - 1). \tag{5.6}$$

The $-\kappa^2$ term indicates that the mode with $\kappa = 0$ is the most unstable one: If the fixed point is stable respect to perturbations with $\kappa = 0$, then it is also stable with respect to all perturbations $\kappa > 0$. Note that the inhomogeneous mode depends on m_l only.

While these results have been correctly stated in [10], there is an interesting case that had been overlooked there: the obvious choice $m_l = 0$ (thus corresponding to the case of purely global feedback, since $m_l + m_g = 1$). In this case, the eigenvalue of the inhomogeneous mode becomes

$$\lambda = 1 - \mathrm{i}\omega - \kappa^2 - \mathrm{i}\beta\kappa^2, \tag{5.7}$$

which means (a) that the (global) feedback does not have any impact on the stability of the inhomogeneous mode, and (b) that the stationary state is unstable for all perturbations with $\kappa < 1$. Since global stability requires stability with respect to the homogeneous mode and the most critical inhomogeneous mode ($\kappa = 0$), we see that amplitude death is impossible to achieve for $m_l = 0$ and that $m_l \neq 0$ is necessary in order to observe amplitude death, being $m_l = 1$ the most favorable case. As a matter of fact, this agrees completely with simulations shown in Figure 2 of [12] where the area of amplitude death is largest for $m_l = 1$, decreases for smaller m_l, and is eventually absent for $m_l = 0$.

We need not to stop here and observe that all critical curves of (5.6) for $\kappa = 0$ and different m_l lie *within* the area where $H = 0$ as given by (5.4). Thus, stability with respect to space-dependent perturbations is obtained only if the system is already stable with respect to uniform perturbations. Therefore, we can actually go beyond the analysis of [10] and can revise the equations for the inhomogeneous modes taking into account that in the case of criticality $H = 0$ within the equations for $A_\pm$. We obtain to lowest order

$$\begin{aligned}
\dot{A}_+ &= (1 - \mathrm{i}\omega)A_+ - (1 + \mathrm{i}\alpha)(|A_+|^2 + 2|A_-^*|^2)A_+ - (1 + \mathrm{i}\beta)\kappa^2 A_+ \\
&\quad + \mu m_l e^{\mathrm{i}\xi}(A_+(t - \tau) - A_+), \qquad (5.8a) \\
\dot{A}_-^* &= (1 + \mathrm{i}\omega)A_-^* - (1 - \mathrm{i}\alpha)(|A_-^*|^2 + 2|A_+|^2)A_-^* - (1 - \mathrm{i}\beta)\kappa^2 A_-^*
\end{aligned}$$

$$+ \mu m_l e^{-\mathrm{i}\xi}(A_-^*(t-\tau) - A_-^*). \tag{5.8b}$$

This is also the lowest order at which the two modes are coupled. Of course, if we assume $|A_\pm| \ll 1$, we recover the decoupled system (5.2b), 5.2c studied above. More interestingly, if we neglect the time-delay terms and the term proportional to κ, the system reduces to the normal form of a Hopf bifurcation with circular symmetry [5, 6]. This equation is known to have either standing or traveling waves as fundamental solutions, depending on the prefactors of the cubic terms, generally to be of the form $a|A_+|^2 + b|A_-^*|^2$. If $b > a > 0$ – as in our case – traveling waves are a stable solution of (5.8). Indeed, traveling waves of small amplitude (around $< 10^{-4}$) were observed in a number of simulations performed close to the area of amplitude death ([12] and unpublished results) which suggest that they were created in this scenario.

6. Conclusion

Following previous work [12, 10, 11], a complex Ginzburg-Landau equation subjected to local and global time-delay feedback terms has been considered. In particular, we have revisited the multiple oscillatory solutions that exist in this model. First result was the observation that the amplitude of a limit cycle can vanish (and hence the limit cycle disappear) while the frequency solution still suggests a valid solution. Secondly, we have derived several analytical criteria for the disappearance of limit cycle solutions, frequency degeneration, amplitude degeneration, and frequency extrema. Only the frequency degeneration condition had been mentioned in previous work [10], albeit not in detail. This gives us the possibility to select for limit cycles with desired properties, e.g., for birhythmicity where the limit cycles should have a maximum difference in frequency and minimum difference in amplitude. Then, we have discussed the influence of the phase shift parameter ξ, which in previous work had always taken a fixed value $\xi = \pi/2$. In principle, ξ can be chosen freely between 0 and 2π, but we point out some invariances and symmetries for ξ. Finally, we discuss the phenomenon of amplitude death, the stabilization of the steady state and the decay of all oscillations. Going beyond the analysis in [10], we show that amplitude death cannot happen if $m_l = 0$, i.e., for global feedback only. In the parameter space (τ, μ) where the stationary state is stable with respect to homogeneous perturbations, but unstable with respect to inhomogeneous perturbations, we predict the onset of traveling wave patterns.

Acknowledgments

M. S. acknowledges very gratefully many discussions and continuous support by Alfonso Casal.

References

[1] I. S. Aranson, L. Kramer; The world of the complex Ginzburg-Landau equation. *Rev. Mod. Phys.*, 74:99–143, 2002.

[2] C. Beta, A. S. Mikhailov; Controlling spatiotemporal chaos in oscillatory reaction-diffusion systems by time-delay autosynchronization. *Physica D*, 199:173–184, 2004.

[3] A. C. Casal, J. I. Díaz; On the complex Ginzburg-Landau equation with a delayed feedback. *Math. Mod. Meth. App. Sci.*, 16:1–17, 2006.

[4] A. C. Casal, J. I. Díaz, M. Stich; On some delayed nonlinear parabolic equations modeling CO oxidation. *Dyn. Contin. Discret. Impuls. Syst. A*, 13 (Supp S):413–426, 2006.

[5] M. C. Cross, P. C. Hohenberg; Pattern formation outside of equilibrium. *Rev. Mod. Phys.*, 65:851–1112, 1993.
[6] G. Danglmayr, L. Kramer; Mathematical tools for pattern formation. In F. Busse and S. C. Müller, editors, *Evolution of spontaneous structures in dissipative continuous systems*, pages 1–85. Springer, Berlin, 1998.
[7] Y. Kuramoto; *Chemical Oscillations, Waves, and Turbulence*. Springer, Berlin, 1984.
[8] A. S. Mikhailov, K. Showalter; Control of waves, patterns and turbulence in chemical systems. *Phys. Rep.*, 425:79–194, 2006.
[9] E. Schöll, H. G. Schuster, editors; *Handbook of Chaos Control*. Wiley-VCH, Weinheim, 2007.
[10] M. Stich, C. Beta; Control of pattern formation by time-delay feedback with global and local contributions. *Physica D*, 239:1681–1691, 2010.
[11] M. Stich, A. Casal, C. Beta; Stabilization of standing waves through time-delay feedback. *Phys. Rev. E*, 88:042910, 2013.
[12] M. Stich, A. C. Casal, J. I. Díaz. Control of turbulence in oscillatory reaction-diffusion systems through a combination of global and local feedback. *Phys. Rev. E*, 76:036209, 2007.

Michael Stich
Non-linearity and Complexity Research Group, School of Engineering and Applied Science, Aston University, Aston Triangle, Birmingham B4 7ET, UK
E-mail address: m.stich@aston.ac.uk